# Gain Enhancement Planar Lens Antenna based on Wideband Focusing Gradient Meta-surface

**Qiming Yu, Shaobin Liu, Zhengyu Huang, Xiangkun Kong, Yuehong Hu, and Yongdiao Wen**

College of Electronic and Information Engineering
Nanjing University of Aeronautics and Astronautics, Nanjing, 211106, China
yqm1604504@nuaa.edu.cn, lsb@nuaa.edu.cn, huangzynj@nuaa.edu.cn, xkkong@nuaa.edu.cn,
1961540605@qq.com, flymew@126.com

***Abstract*** ─ A three-layered transmitting focusing gradient meta-surface (FGMS) has been proposed, which can achieve broadband gain enhancement from 8.2 GHz to 10 GHz. The element of broadband transmitting FGMS has high transmitting efficiencies that over 0.7 and achieve [0, 2π] phase range with a flat and linear trend in the operating band. The FGMS can transform the spherical waves into plane waves. Three patch antennas working at 8.2 GHz, 9.1 GHz, and 10 GHz respectively are placed the focus of broadband FGMS as the spherical-wave source to build a broadband planar lens antenna system. It achieves a simulation gain of 15.44 dBi which is 7.51dB higher than that of the bare patch antenna at 10 GHz with satisfying SLLs and beamwidths. However, it enhanced the gain of the bare patch antenna in a wide operating band. Finally, the FGMS and the patch antenna are fabricated and measured. The measured results are in good agreement with the simulations.

***Index Terms*** ─ Broadband gain enhancement, focusing gradient meta-surface, lens antenna, transmissive.

## I. INTRODUCTION

Nowadays, meta-surfaces as a class of metamaterials that have been widely studied [1-4]. As a two-dimensional material in metamaterials, it has many advantages, such as low profile, easy manufacturing, miniaturization, ease to conformal, etc. The gradient meta-surface is the most research-worthy category, which can manipulate the phase and polarization of the wave to control the phase and amplitude. So far, gradient meta-surface has been greatly developed and applied in the microwave field, which can achieve the functions of polarization split [5], radar cross-section reduction [6], anomalous refraction/reflection [7], transformation [8], and focusing [9].

The phase gradient meta-surface (PGMS) is a subclass of MS which has been proposed by Yu [10]. The focusing GMS (FGMS) can transform spherical wave to plane wave, but the point source should be placed at the focal point of the PGMS. Due to the reciprocity of electromagnetic waves, vice versa. This performance can be used in the design of a high gain planar lens antenna by placing the feed antenna at the focus of the FGMS [11-13].

Lens antennas have a wide range of applications in remote wireless communication systems, which effectively combines the advantages of parabolic antennas and phased array antennas to produce extremely high gains. Lens antennas employing meta-surfaces such as zero/low index metamaterial [14] or gradient-refractive-index metamaterial [15] have been heavily researched. Reflect-array [16] and transmit-array [17] antennas have received extensive attention because of their simple structure and thinness. A high-gain transmitting lens antenna by employing layered phase-gradient meta-surface (MS) has been proposed [18]. The meta-surface is engineered to focus the propagating plane wave to a point with high efficiency. A single-layer focusing gradient meta-surface built by one element-group has been proposed [19]. The lens antenna achieves a pencil-shaped radiation pattern with a simulation maximum gain of 16.7dB at 10GHz. But today's lens antennas are mostly narrowband, can't meet the needs of remote wireless communication systems. Therefore, it is necessary to develop a broadband high gain lens based on FGMS.

In this work, a three-layered transmitting FGMS has been proposed, which can achieve broadband gain enhancement from 8.2 to 10GHz.The broadband transmitting FGMS element requires stable phase compensation, high transmit efficiency, and the phase of the phase-shifting element changes flatly and linearly in the wide frequency band. Then elements with different types and compensation phases are located on the surface according to the hyperbolic phase distribution to build broadband focusing FGMS. The FGMS can transform the spherical waves into plane waves, which can be used to build a planar lens antenna. Three patch antennas working at 8.2 GHz, 9.1 GHz, and 10 GHz respectively are placed the focus of broadband FGMS as the

*Submitted On: October 31, 2018*
*Accepted On: July 6, 2021*
https://doi.org/10.47037/2020.ACES.J.360605

spherical-wave source to build a broadband planar lens antenna system, that enhanced the gain of the bare patch antenna in a wide operating band.

## II. MULTILAYER TRANSMITTING FOCUSING GMS DESIGN

### A. Design principle of GMS

The phase gradient meta-surface can be simply divided into two types: transmissive and reflective. Compared with the reflecting FGMS, the design of the transmitting FGMS is more difficult, which requires not only stable phase compensation but also high transmit efficiency. Figure 1 shows the working mechanism of transmitting focusing FGMS. Transmitting focusing FGMS can convert incident plane waves into spherical waves emitted by the source located at its focus and vice versa. This performance can be used in the design of a high gain planar lens antenna by placing the feed antenna at the focus of the FGMS.

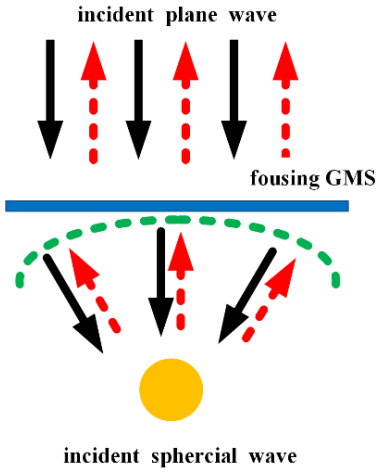


Fig. 1. The schematics of focusing FGMS. The green dashed line shows the hyperbolic phase distribution of the meta-surface given by Eq. (1).

Usually the phase distribution of the focused FGMS unit obeys the hyperbolic formula:

$$\Phi(x,y)=\frac{2\pi}{\lambda_0}\left(\sqrt{x^2+y^2+L^2}-L\right)+\Phi_0, \qquad (1)$$

where $L$ is the focal length of the lens, $\lambda_0$ is the free space wavelength, $x$ and $y$ are the position coordinate of the lens unit on the lens. When the plane incident waves perpendicular to the transmitting focusing FGMS, the transmitted electromagnetic wave is deflected toward the phase delay direction. The anomalous refraction can be explained by the generalized law of refraction, which is defined by the following formula:

$$n_t sin(\theta_t)-n_i sin(\theta_i)=\frac{\lambda}{2\pi}\frac{d\phi}{dx}, \qquad (2)$$

where $\phi$ is the phase distribution of the focused FGMS unit, $n_t$ and $n_i$ are the refractive index of the refracted medium and incident medium, $\theta_t$ and $\theta_i$ are the refracted and incident angle of electromagnetic wave, $\lambda$ is the wavelength of electromagnetic waves:

$$d\phi/dx=2\pi/np, \qquad (3)$$

where $n$ is the number of phase shifting elements for constructing the supercell of FGMS. In this design, the entire transmitting FGMS is placed in an air box, so $n_t = n_i=1$,

$$\theta_t=sin^{-1}\left(\frac{\lambda}{2\pi}\times\frac{2\pi}{np}\right). \qquad (4)$$

When the element has achieved [0, 2π] phase range, a transmitting focusing FGMS that regulates the transmission direction of the electromagnetic wave can be obtained by designing a reasonable phase gradient and arranging the elements into an array.

### B. Element design

Designing broadband transmitting focusing FGMS, in addition to satisfying the two above conditions, it is also required that the transmission phase of the phase-shifting element changes in a flat and linear manner in the operating frequency band. As shown in Fig. 2, the element of meta-surface structure is composed of four metallic layers and three intermediate dielectric layers, each metallic layer contains a square ring outside and a square patch inside. the dielectric substrate is F4b, which has a permittivity of 2.65, a thickness of 2.5 mm, and a loss tangent of 0.001. To efficiently control the phase gradient, the side length of the inside square patch is chosen to vary while fix $a$=8mm, $l$=7.9 mm, $w$=0.1 mm, $d$=2.5 mm. So, the total thickness of the FGMS is 7.5 mm.

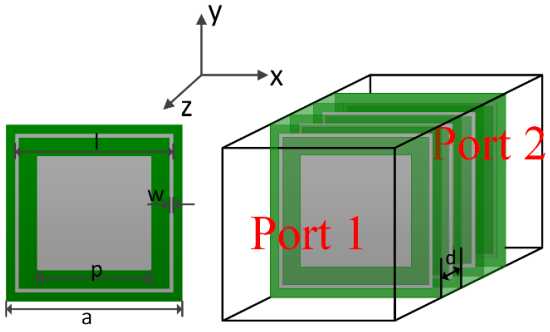


Fig. 2. Structure of the FGMS element and the simulated setup. (a) Top view; (b) perspective view.

Figure 3 shows the transmission coefficients of a phase-shifting element with different $p$. In the 8.2~10GHz frequency band, the amplitude of the transmission coefficient curve ranges from 0.7 to 1 as the change of square patch length. It indicates that the designed element of FGMS has a relatively large transmissivity. Figure 4

shows the phase of $S_{21}$ for which indicates that the phase range. The three layers element has achieved [0, 2π] phase range with a flat and linear trend in the operating band. It satisfies the requirement for transmitting FGMS design.

A supercell that provides a linear phase gradient has been designed, which can manipulate the EM waves effectively. The supercell is composed of seven elements. The inside square metal patch side (*p*) of each element has a length of 7.2mm, 7mm, 6.6mm, 6.2mm, 5.7mm, 4.8mm, 4mm from large to small, meanwhile the other parameters of the elements remain unchanged. Each phase-shifting element can compensate for the phase of 51.43°.

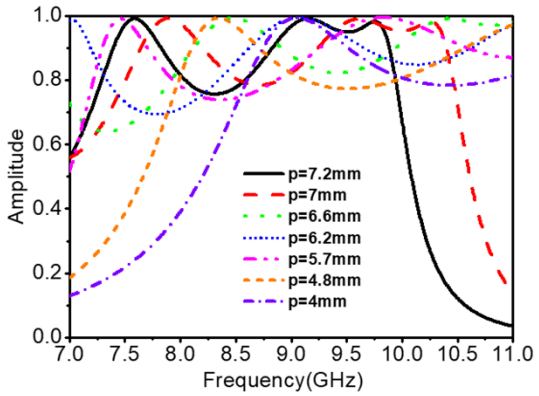


Fig. 3. Transmission coefficients of phase shifting element with different value of *p*.

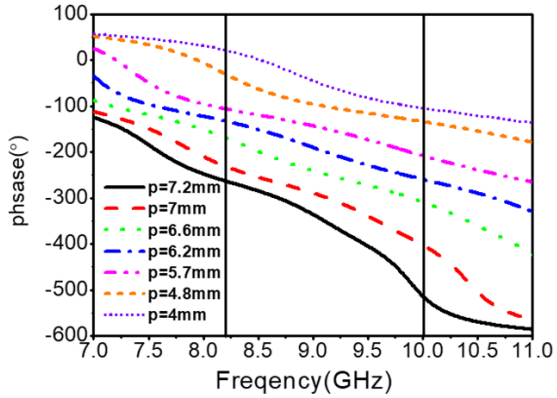


Fig. 4. Transmission phases of the seven elements with different value of *p*.

### C. Focusing GMS design

In the previous part, a supercell, that can cover enough phase range with high transmitting efficiencies, has been designed. The supercell, that composed of seven different phase compensation elements, is used for building a (two- dimensional) 2D focusing FGMS. To determine the phase that needs to be compensated for each element position on the plane of the FGMS, equation (1) can be written as follows:

$$\Delta\varphi(m,n)=\frac{2\pi}{\lambda_0}\left(\sqrt{(mp)^2+(np)^2+L^2}-L\right)+2k\pi\,, \quad (5)$$

where k=0,1,2…, *m* (*n*) is the number of the element in *x*(*y*)-direction, $\Delta\varphi$ (m, n) is the phase difference between the element placed at the location of (mp, np) and the element placed at the origin (m=0, n=0).

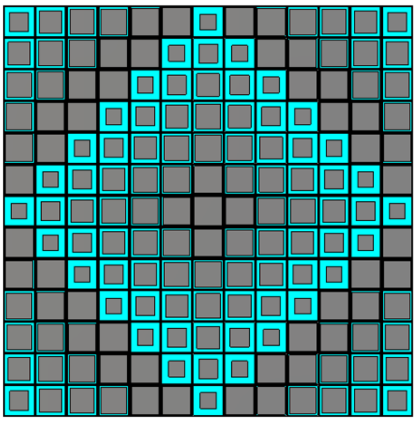

Fig. 5. The prototype of designed planar transmission type focusing FGMS.

We use 7 elements to cover about 2π phase shift which was mentioned above. Figure 5 shows the prototype of the designed planar transmission type focusing FGMS, which with elements of 13×13 and a size of 104mm×104mm. Due to the central symmetry of the distribution of FGMS phase-shifting element and the symmetry of element, so the designed wideband FGMS is polarization insensitive. To yield the focusing phenomenon, a plane wave is located 20mm over the MS to illuminate it. Figure 6 shows the focusing effect of the proposed design FGMS. The simulated electric field (Ex) amplitude distributions on xoz-plane at 8.2GHz, 9.1GHz, and 10GHz have been shown. The power densities on the xoz-plane have been focused on a spot. Due to the polarization insensitivity of the FGMS structure, the same behavior exists in the yoz-plane.

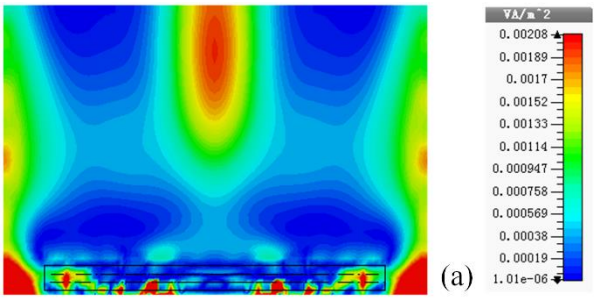


(a)

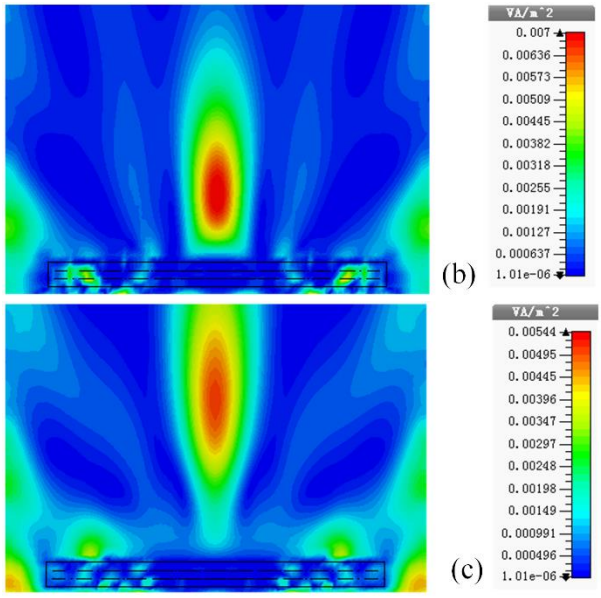


Fig. 6. Focusing effect of the proposed design FGMS. Simulated electric field (Ex) amplitude distributions on *xoz*-plane. (a) 8.2 GHz; (b) 9.1 GHz; (b) 10 GHz.

## III. HIGH-GAIN LENS ANTENNA APPLICATION

We can design a wideband, gain enhancement planar lens antenna operating at X-band based on the designed FGMS. The proposed FGMS can transform the spherical wave emitted by the patch antenna to a near-plane wave, which enables gain enhancement. The schematic of the lens antenna is shown in Fig. 7. A patch antenna has been located 30mm away from the FGMS to feed the FGMS. The antenna placement position needs to be close to the focus of FGMS. Three patch antennas are designed to verify the gain effect of wideband lenses based on FGMS. An antenna structure as shown in Fig. 7, radiant surface is a round metal patch and coaxial feed has been used. The substrate is F4b, which has a permittivity of 2.65 and a loss tangent of 0.001.

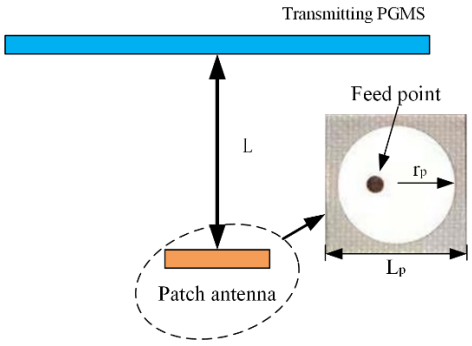


Fig. 7. The schematic of the lens antenna.

Three patch antennas working at 8.2 GHz, 9.1 GHz, and 10 GHz respectively are designed and the measured reflection coefficients with and without the FGMS are shown in Fig. 8. It can be seen from Fig. 8 that the resonant frequency band of the antenna is deviated after loading the lens, mainly due to the existence of parasitic coupling between the radiation source antenna and the FGMS. The measured results are in good agreement with the simulation results.

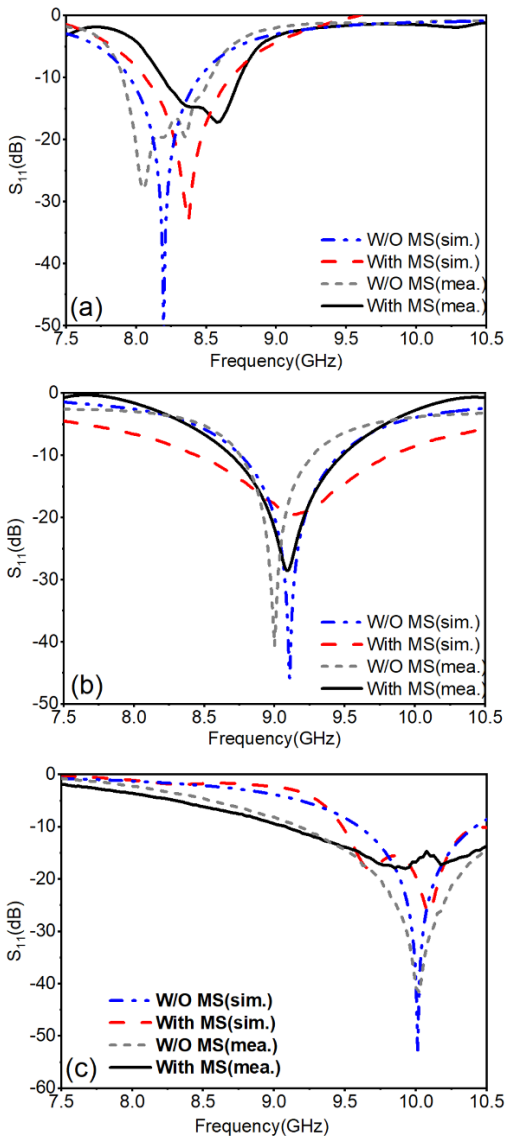


Fig. 8. $S_{11}$ of three patch antennas with and without loading the FGMS. (a) 8.2GHz; (b) 9.1GHz; (c) 10 GHz.

Figures 9 (a) and (b) show the sample of lens antenna with FGMS. Hard foam of the thickness of 30mm has been loaded between patch antenna and

FGMS to fix patch antenna and FGMS. Figure 9 (c) shows the test scenario of an anechoic chamber.

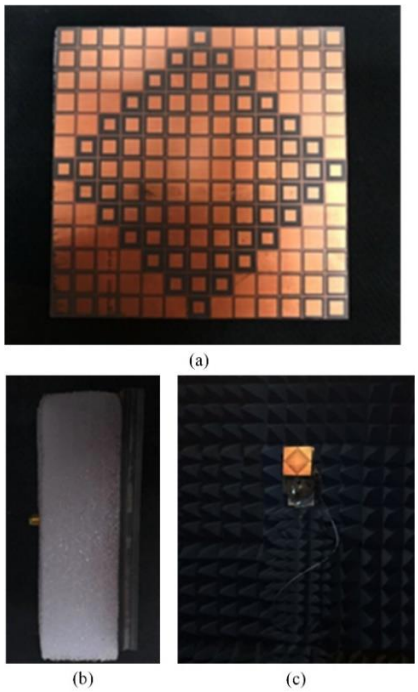


Fig. 9. The sample of lens antenna with FGMS. (a) Front view; (b) side view; (c) the test scenario of anechoic chamber.

To demonstrate the performances of the system more clearly, we display the far-field radiation patterns of the patch antenna with and without the FGMS at 8.2GHz, 9.1GHz, and 10GHz of two orthogonal planes in Fig.10.

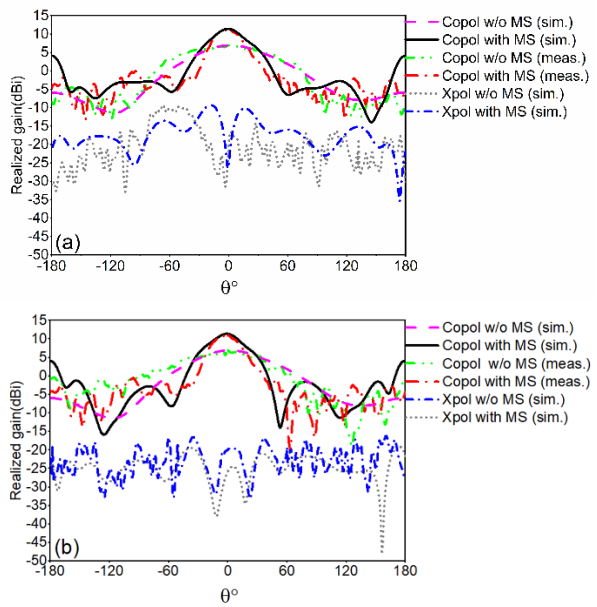


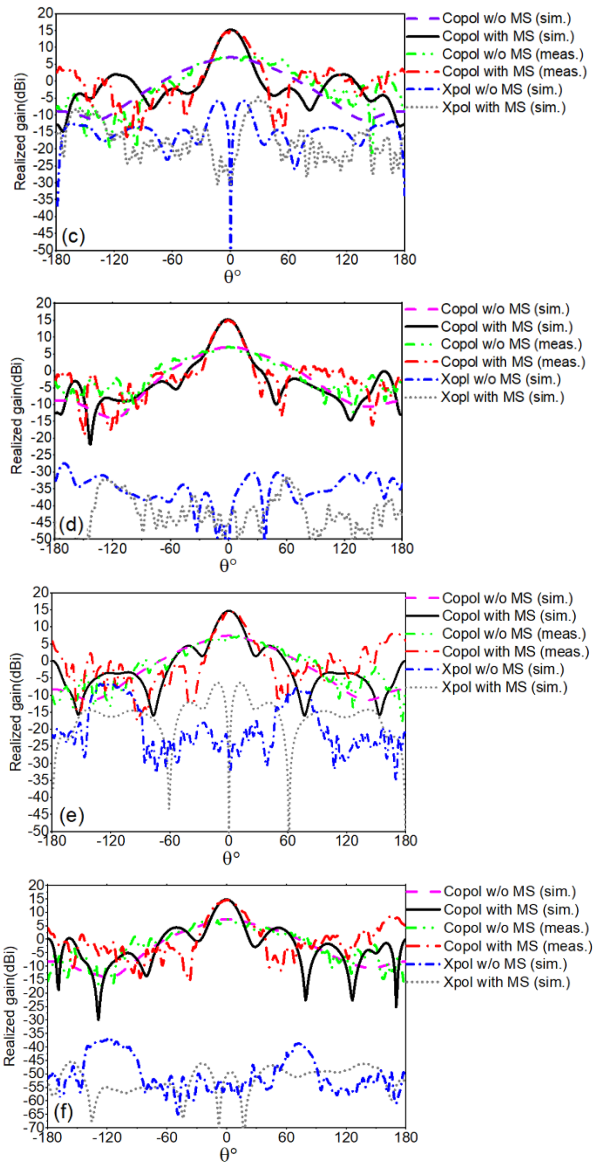


Fig. 10. Simulated and measured far-field radiation patterns of the patch antenna with and without the FGMS. (a) 8.2 GHz, *xoz*-plane; (b) 8.2 GHz, *yoz*-plane; (c) 9.1 GHz, *xoz*-plane; (d) 9.1 GHz, *yoz*-plane; (e) 10 GHz, *xoz*-plane; (f) 10 GHz, *yoz*-plane.

As is shown in Figs. 10 (a) and (b), the lens antenna has a simulation gain of 11.92 dBi which is 5.15dB higher than that of the bare patch antenna at 8.2 GHz. The measured peak gain is 11.04 dBi which is 4.66 dB higher than that of the bare patch antenna at 8.2 GHz. As is shown in Figs. 10 (c) and (d), the lens antenna has a simulation gain of 15.60 dBi which is 8.44 dB higher than that of the bare patch antenna at 9.1 GHz. The measured maximum gain is 14.9 dBi which is 7.54 dB higher than that of the bare patch antenna at 9.1 GHz. As shown in Figs. 10 (e) and (f), the lens antenna has a

simulation gain of 15.44 dBi which is 7.51dB higher than that of the bare patch antenna at 10 GHz. The measured peak gain is 14.26 dBi which is 6.66 dB higher than that of the bare patch antenna at 10 GHz. Compared with the measured results, the simulation results are about 1dB higher, which is acceptable by considering the possible machining errors and test errors.

In the case of the pure patch antenna without adding the lens, the antenna efficiency of 89.5% is obtained at 9.1GHz. Note that the aperture efficiency is evaluated with respect to the utmost directivity which can be calculated through the equation:

$$\eta = G / D_{\max} = G / \left(4\pi PQ / \lambda_0^2\right) \times 100\%, \qquad (6)$$

with $P$ = 104 mm and $Q$ = 30 mm is the length and width of the focusing meta-surface, respectively. In the case of the patch antenna with adding the lens, the antenna efficiency of 41% is obtained at 9.1GHz.

The lens antenna based on FGMS designed in this paper has been proven to achieve gain enhancement over a wide range of frequencies from 8.2 to 10GHz. In addition, small overall size with less number of elements inevitably brings a decrease in the peak gain.

Table 1: Comparison of the performances between previous literature and this work

| Ref. | WF *f*/GHz | Aperture Efficiency | F/D Ratio | Unit Cell Number |
|---|---|---|---|---|
| [18] | 10 | 31.4% | 0.19 | 196 |
| [19] | 9.9-10.2 | N.A. | 0.29 | 144 |
| [20] | 15-18 | 6.17% | 0.43 | 576 |
| [21] | 9.275 | 56.3% | 0.8 | 121 |
| This work | 9.1-10 | 41% | 0.28 | 144 |

WF=Working Frequency.

The comparisons between the results of this work with earlier transmit-arrays are shown in the following Table 1. From the Table 1, we can see that the designed lens antenna has good performance in terms of antenna working bandwidth and aperture efficiency. The proposed lens antenna has a smaller F/D ratio, which will facilitate the requirements of low-profile antennas. In addition, fewer units cell number of transmit-arrays mean easier processing and lower costs.

## IV. CONCLUSION

In conclusion, a gain enhancement broadband planar lens antenna operating from 8.2GHz to 10GHz based on wideband focusing gradient meta-surface is simulated, fabricated, and measured. The prototype of the designed planar transmission type focusing FGMS has elements of 13×13 and a size of 104 mm×104 mm×7.5 mm. High transmitting efficiencies of the elements, the phase of the phase-shifting element changes with a flat and linear manner in a wide frequency band, and a good focusing effect of the FGMS guarantee the good performances of the broadband transmitting lens antenna. It achieves a simulation gain of 15.44 dBi which is 7.51dB higher than that of the bare patch antenna at 10 GHz with satisfying SLLs and beamwidths. Moreover, the gain is improved from 8.2GHz to 10 GHz, which implements broadband FGMS.

## ACKNOWLEDGMENT

This work was supported by National Natural Science Foundation of China (Grant No. 62071221, 62071442), Postgraduate Research & Practice Innovation Program of Jiangsu Province (Grant No. KYCX19_0189), China Scholarship Council (Grant No. 201906830067).

## REFERENCES

[1] J. Zhao, B. Li, Z. N. Chen, and C. W. Qiu, "Redirection of sound waves using acoustic metasurface," *Appl. Phys. Lett.*, vol. 103, no. 15, p. 151604, 2013.

[2] Y. Li, J. Zhang, S. Qu, J. Wang, H. Chen, Z. Xu, and A. Zhang, "Wideband radar cross section reduction using two-dimensional phase gradient metasurfaces," *Appl. Phys. Lett.*, vol. 104, no. 22, p. 221110. 2014.

[3] X. Wan, W. X. Jiang, H. F. Ma, and T. J. Cui, "A broadband transformation-optics metasurface lens," *Appl. Phys. Lett.*, vol. 104, no. 15, p. 151601, 2014.

[4] C. Saeidi and D. Weide, "Wideband plasmonic focusing metasurfaces," *Appl. Phys. Lett.*, vol. 105, no. 5, p. 053107. 2014.

[5] T. Cai, G. M. Wang, X. F. Zhang, J. G. Liang, Y. Q. Zhuang, D. Liu, and H. X. Xu, "Ultra-thin polarization beam splitter using 2-D transmissive phase gradient metasurface," *IEEE Trans. Antennas Propagat.*, vol. 63, no. 12, pp. 5629-5636. 2015.

[6] Y. Li, J. Zhang, S. Qu, J. Wang, H. Chen, Z. Xu, and A. Zhang, "Wideband radar cross section reduction using two-dimensional phase gradient metasurfaces," *Appl. Phys. Lett*, vol. 104, no. 22, p. 221110, 2014.

[7] Z. Wei, Y. Cao, X. Su, Z. Gong, Y. Long, and H. Li, "Highly efficient beam steering with a transparent metasurface," *Opt. Express*, vol. 21, no. 9, pp. 10739-10745, 2013.

[8] C. Pfeiffer and A. Grbic, "Bianisotropic metasurfaces for optimal polarization control: Analysis and synthesis," *Phys. Rev.* A, vol. 2, no. 4, p. 044011, 2014.

[9] F. Monticone, N. M. Estakhri, and A. Alù, "Full control of nanoscale optical transmission with a composite metascreen," *Phys. Rev. Lett.*, vol. 110, no. 20, p. 203903. 2013.

[10] N. Yu, P. Genevet, M. A. Kats, F. Aieta, J. P. Tetienne, F. Capasso, and Z. Gaburro, "Light

propagation with phase discontinuities: Generalized laws of reflection and refraction," *Science*, pp. 333-337, 2011.

[11] A. Belen, P. Mahouti, F. Güneş, and Ö Tari, "Gain enhancement of a traditional horn antenna using 3D printed square-shaped multi-layer dielectric lens for X-band applications," *Appl. Comput. Electromagn. Soc. J.*, vol. 36, no. 2, pp. 132-138, 2021.

[12] A. Belen and E. Tetik, "Realization of modified elliptical shaped dielectric lens antenna for X band applications with 3D printing technology," *Appl. Comput. Electromagn. Soc. J.*, vol. 35, no. 8, pp. 916-921, 2020.

[13] S. Loredo, G. León, O. F. Robledo, and E. G. Plaza, "Phase-only synthesis algorithm for transmitarrays and dielectric lenses," *Appl. Comput. Electromagn. Soc. J.*, vol. 33, no. 3, pp. 259-264, 2018.

[14] H. X. Xu, G. M. Wang, and T. Cai, "Miniaturization of 3-D anistropic zero-refractive-index metamaterials with application to directive emissions," *IEEE Trans. Antennas Propagat.*, vol. 62, no. 6, pp. 3141-3149, 2014.

[15] H. X. Xu, G. M. Wang, Z. Tao, and T. Cai, "An octave-bandwidth half Maxwell fish-eye lens antenna using three-dimensional gradient-index fractal metamaterials," *IEEE Trans. Antennas Propagat.*, vol. 62, no. 9, pp. 4823-4828, 2014.

[16] R. S. Malfajani and Z. Atlasbaf, "Design and implementation of a dual-band single layer reflectarray in X and K bands," *IEEE Trans. Antennas Propagat.*, vol. 62, no. 8, pp. 4425-4431, 2014.

[17] A. H. Abdelrahman, A. Z. Elsherbeni, and F. Yang, "Transmitarray antenna design using cross-slot elements with no dielectric substrate," *IEEE Antennas Wireless Propag. Lett.*, vol. 13, pp. 177-180, 2014.

[18] H. Li, G. Wang, H. X. Xu, T. Cai, and J. Liang, "X-band phase-gradient metasurface for high-gain lens antenna application," *IEEE Trans. Antennas Propagat.*, vol. 63, no. 11, pp. 5144-5149, 2015.

[19] H. Li, G. Wang, J. Liang, X. Gao, H. Hou, and X. Jia, "Single-layer focusing gradient metasurface for ultrathin planar lens antenna application," *IEEE Trans. Antennas Propagat.*, vol. 65, no. 3, pp. 1452-1457, 2017.

[20] H. Hai-Sheng, W. Guang-Ming, L. Hai-Peng, C. Tong, and G. Wen-Long, "Ultra-thin broadband flat metasurface to focus electromagnetic waves and its application in high-gain antenna," *Acta Physica Sinica*, vol. 65, no. 2, 2016.

[21] X. Zhao, C. Yuan, L. Liu, S. Peng, Q. Zhang, and H. Zhou, "All-metal transmit-array for circular polarization design using rotated cross-slot elements for high-power microwave applications," *IEEE Trans. Antennas Propagat.*, vol. 65, no. 6, pp. 3253-3256, 2017.

**Qiming Yu** was born in Zhejiang Province, China, in 1992. He received the B.S. degree and M.S. degree from Nanchang University, Nanchang, China, in 2014 and 2016, respectively. He is currently pursuing the Ph.D. degree in Nanjing University of Aeronautics and Astronautics, Nanjing, China. His current research interests include frequency selective surface, rasorber and lens antenna.

**Shaobin Liu** received the Ph.D. degree in Electronics Science and Technology from the National University of Defense Technology in 2004. However, in 2003, he was already promoted as Professor. He is currently a Professor of Electromagnetic and Microwave Technology at the Nanjing University of Aeronautics and Astronautics. His research focuses on plasma stealthy antennas, frequency selective surface and absorber, rasorber, radio frequency, electromagnetic compatibility.